OPTICAL REVIEW Vol. 11, No. 3 (2004) 1–5

A Wavelength and Spectrum Measurement of an Extremely-Short-External-Cavity Laser Diode by Precisely Controlling Slider Flying Height

Hiroo UKITA* and Yoshinobu KARAKI

Faculty of Science and Engineering, Ritsumeikan University, 1-1-1, Nojihigashi, Kusatsu-shi, Shiga, 525 Japan

(Received December 5, 2003; Accepted February 17, 2004)

In this paper we propose a measurement method that uses a laser diode (LD) attached to a flying slider and a semi-transparent rotating disk mirror for an extremely-short-external-cavity configuration. Not only the wavelength, but also the spectrum and the light output are measured at room temperature with the external cavity length, the reflectivities of the LD facets and the external mirror, and the drive current as parameters. We have confirmed wavelength variation as great as 30 nm by changing the external-cavity length for a 1.3-μm wavelength laser diode with an antireflection coating on the LD facet facing the external mirror.

Key words: extremely short external cavity, laser diode, flying slider, wavelength variation, spectrum, external-cavity length, antireflection coating

1. Introduction

Extremely-short-external-cavity laser diodes (ESEC LDs) have been demonstrated for monitoring reflectivity[1] or displacement.[2] Tunable laser diodes[3] are also demonstrated for ESEC configuration. ESEC LDs include desirable properties for optical communications, optical data storage, spectroscopy, and a variety of sensing and measurement systems.

A surface-emitting laser diode with a micromechanical reflector can be used for tuned devices.[4–6] The structure is designed to have an air-gap of about one wavelength. When a voltage is applied to the membrane reflector, the electrostatic force reduces the air-gap, which changes the wavelength. An edge-emitting laser diode is also available for the micromechanically tunable laser.[7,8] By varying the external cavity length, the laser wavelength can be easily changed. However, the experimental data of the ESEC LD for various coupled conditions have been poor till now.

Some studies have reported special considerations for such a short-external-cavity laser diode based on butt coupling into an optical fiber.[6,9] In a short-external-cavity LD system, the feedback light must return to an approximately 1-μm laser diode aperture, although it is difficult in practice to align the light beam with such micrometer-level accuracy, and it is more difficult to maintain this accuracy for a long period against external environmental perturbations.[10] One possible solution is automatic alignment using an air bearing slider which has the same flying mechanism as that of a hard disk drive (HDD).

In this paper we demonstrate how to measure the effect of the feedback light for an extremely-short-external-cavity (2 to 4.5 μm) laser diode configuration, using the external cavity length, the reflectivity of the LD facet facing the external mirror, the reflectivity of the external mirror, and the drive current as parameters.

*E-mail address: ukita@se.ritsumei.ac.jp

2. Measuring Method

2.1 General description

Some aspects of the feedback effect for an ESEC LD configuration were measured by the following method. An extremely-short external cavity was realized when a laser diode on a slider flew on a semi-transparent optical disk. Figure 1(a) illustrates the experimental setup (upside down in reality) for monitoring the wavelength-related behavior of a laser diode (LD) by an integrated photodiode (PD) which is attached to a flying slider. The InGaAsP/InP LD is isolated from the PD by reactive ion beam etching. The cavity length of the LD is 300 μm and the space between the LD and the PD is 5 μm. The monitor current sensitivity is 0.1 mA/mW. Figure 1(b) shows a photograph of an air-bearing slider with an LD-PD chip.

Automatic and stable alignment is accomplished by the air bearing, which maintains a spacing ranging from sub-micrometers up to several micrometers depending on the disk velocity. The spacing $L_{ex}{}^0$ varies according to the square root of the disk velocity. The external cavity length L_{ex} ($= L_{ex}{}^0 + L_{ex}{}^1$) is 2 to 4.5 μm long in this experiment, where $L_{ex}{}^0$ is the flying height depending on the disk

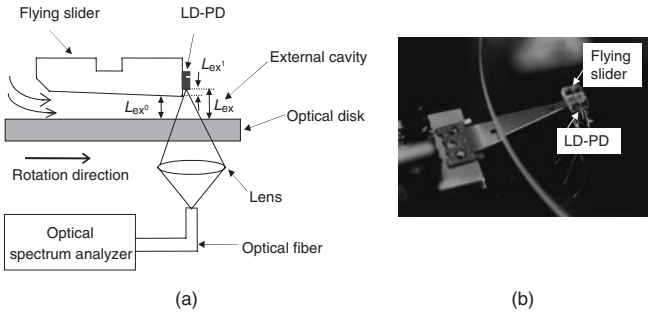

Fig. 1. (a) Proposed setup for measurement of wavelength tuning based on extremely-short external cavity (ESEC) length. A laser diode (LD) attached to an air-bearing slider flies by air resistance caused by disk revolution (upside down in reality). (b) Photograph of the air-bearing slider and an optical disk.

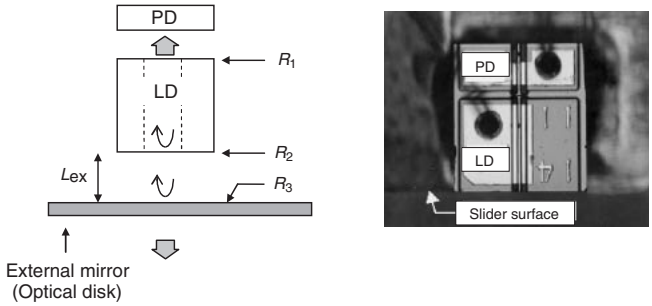

Fig. 2. (a) Detailed representation of the ESEC LD system, and (b) photograph of a monolithically integrated LD-PD chip on a slider.

velocity and $L_{ex}{}^{1}$ is an LD-PD attachment error to the slider surface.

Light transmitted through the semi-transparent disk is directed into an optical spectrum analyzer through an optical fiber placed opposite to the LD-PD. The laser spectrum is observed with the spectrum analyzer (Anritsu, MS96A) with a resolution of 0.1 nm. The corresponding laser power variation is monitored with the PD integrated on the LD.

The laser diode coupled with an optical disk forms a composite cavity LD as shown in Fig. 2(a). Figure 2(b) shows a photograph of the monolithically integrated LD-PD chip on a slider. Optical feedback is varied by the external cavity length (disk rotation rate), the reflectivity of LD facet facing the optical disk and the disk reflectivity itself. In the following, the LD facet reflectivity R_1 is 0.32 (cleaved facet), R_2 is 0.01 (antireflection coating),[11] and the disk reflectivity R_3 are 0.04, 0.26 and 0.50, respectively.

2.2 *Effective reflectivity*

Dependence of lasing characteristics on external-cavity length is described in various parameters: the LD facet reflectivity R_1, the LD facet reflectivity R_2 facing the external mirror, the external mirror reflectivity R_3, and the LD drive current. The external-cavity length L_{ex} also affects the coupling coefficient η which is defined by Eq. (1) as the ratio between the feedback light power $E_z{}^2$ to the original emitted light power $E_0{}^2$, where Gaussian beam waists $(1/e^2)$ at the LD facet are w_{x0} and w_{y0} and $z = 2L_{ex}$.

$$\eta \equiv \frac{\left|\int_{-\infty}^{\infty}\int E_z E_0 \mathrm{d}x\mathrm{d}y\right|^2}{\int_{-\infty}^{\infty}\int |E_z|^2 \mathrm{d}x\mathrm{d}y \int_{-\infty}^{\infty}\int |E_0|^2 \mathrm{d}x\mathrm{d}y} = \frac{\sqrt{\left\{1+\left(\frac{\lambda z}{\pi w_{x0}{}^2}\right)^2\right\}\left\{1+\left(\frac{\lambda z}{\pi w_{y0}{}^2}\right)^2\right\}}}{\left\{2+\left(\frac{\lambda z}{\pi w_{x0}{}^2}\right)^2\right\}\left\{2+\left(\frac{\lambda z}{\pi w_{y0}{}^2}\right)^2\right\}} \quad (1)$$

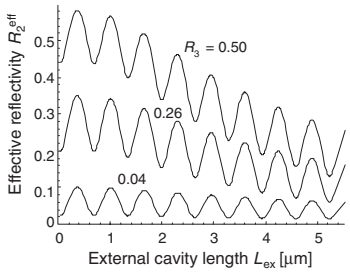

Fig. 3. Dependence of effective reflectivity $R_2{}^{eff}$ on external cavity length L_{ex}.

Effective reflectivity $R_2{}^{eff}$ has been successfully introduced as Eq. (2) to assist understanding of the external-cavity LD lasing characteristics by replacing the LD facet reflectivity R_2 facing the external mirror.

$$R_2{}^{eff} = r_2{}^{eff} r_2{}^{eff*} = \frac{r_2{}^2 + a^2 r_3{}^2 + 2a r_2 r_3 \cos(2\beta_2 L_{ex})}{1 + a^2 r_2{}^2 r_3{}^2 + 2a r_2 r_3 \cos(2\beta_2 L_{ex})} \quad (2)$$

where n_1 is the refractive index of the internal cavity (LD medium), n_2 is that of the external cavity (air), $r_1 = \sqrt{R_1}$, $r_2 = \sqrt{R_2}$, $r_3 = -\sqrt{R_3}$ are the amplitude reflectivities, $\beta_i = 2\pi n_i/\lambda$ is the propagation constant, and $a(= \sqrt{\eta})$ is the amplitude coupling coefficient for the external-cavity length L_{ex}. For a typical LD, Gaussian beam waists $(1/e^2)$ are 1.3 μm and 2.54 μm, dependence of effective reflectivity $R_2{}^{eff}$ on external-cavity length L_{ex} is calculated using Eqs. (1) and (2) as shown in Fig. 3. It is clear from the figure that $R_2{}^{eff}$ changes every half wavelength $(\lambda/2)$.

2.2.1 *Laser diode attachment to a slider*

In order to reduce the attachment error $L_{ex}{}^{1}$ between the LD facet and the slider surface, an LD-PD was mounted on the slider surface by the following method. First, the LD-PD chip was pushed onto the electrode of the slider's back end with vacuum tweezers and then rotated to align it parallel to the slider surface as shown in Fig. 4(a). The parallelism was monitored using a He-Ne laser beam. Second, the moving stage on which the LD-PD chip was mounted was translated, as shown in Fig. 4(b), along the laser beam axis with an accuracy of 0.05 μm to minimize the following error signal.

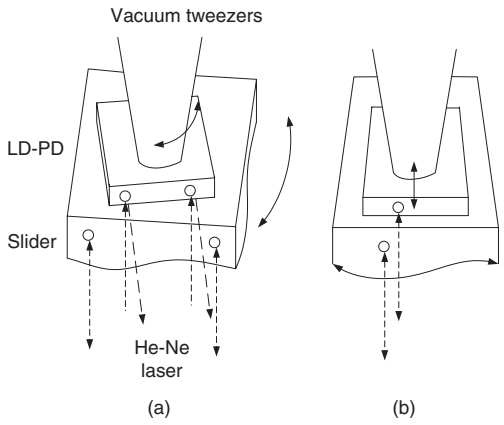

Fig. 4. LD-PD chip bonding method on a slider.

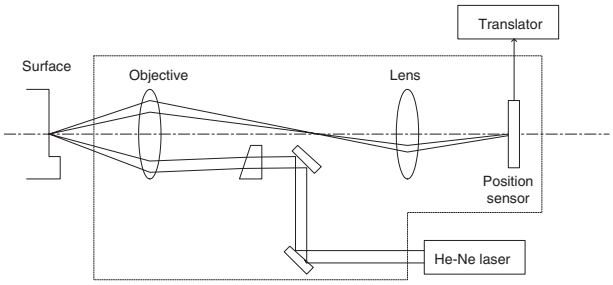

Fig. 5. Auto-focusing geometry for investigating the attachment error $L_{ex}{}^{1}$ between an LD-PD facet and a slider surface. A He-Ne laser incident to the LD-PD facet and the slider surface is reflected back on a position sennsor, transforming the attachment error to the light output difference by a so-called optical lever.

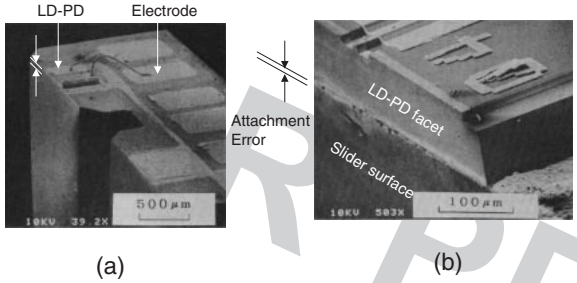

Fig. 6. Photograph of (a) the back end of the slider on which an LD-PD chip is bonded to the electrode and, (b) the LD-PD facet and the slider surface. The attachment error $L_{ex}{}^{1}$ is less than 1 μm.

The attachment error was detected by a range sensor, called an optical lever, as shown in Fig. 5. The light output difference (focus error) between the LD-PD and the slider surface corresponds to the attachment error, and in this experiment the attachment (displacement) error between the two surfaces was less than 1 μm.

Finally, the LD-PD chip was bonded precisely by melting a thin film of solder in H_2-N_2 gas. Figure 6 shows photographs of (a) an LD-PD bonded onto the electrode on the back end of the slider, and (b) an enlarged view of the LD-PD facet and the slider surface.

3. Measured Characteristics

3.1 Light output

In order to analyze the light feedback effects specific to the ESEC LD configuration, we first measured the threshold current. Maximum light output versus drive current (I-L characteristics) with an external mirror is presented in Fig. 7, where $R_1 = 0.32$, $R_2 = 0.01$. The light was detected by the PD placed at the opposite facet of the LD. The threshold current of the ESEC LD with feedback light is significantly reduced for the antireflection-coated LD ($R_2 = 0.01$). These coupled LD operations were calculated for the steady state operation by using the rate equations.

The light output vs. external-cavity-length L_{ex} is shown in Fig. 8, with drive current I/I_{th} as a parameter. The light output coupled to the external mirror depends not only on

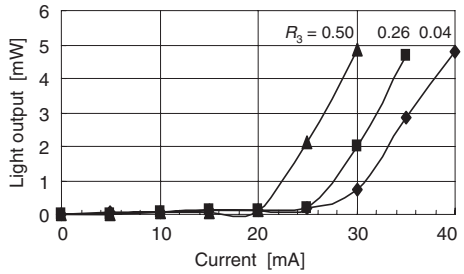

Fig. 7. I-L characteristics with an external mirror at the light-output maxima, external mirror reflectivity R_3 as a parameter, where $R_1 = 0.32$, $R_2 = 0.01$.

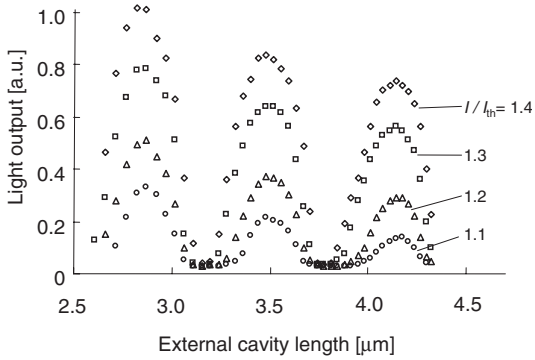

Fig. 8. Light output vs. external cavity length L_{ex} ($= L_{ex}{}^{0} + L_{ex}{}^{1}$), drive current I/I_{th} normalized by threshold current as a parameter, where $R_1 = 0.32$, $R_2 = 0.01$, and $R_3 = 0.5$.

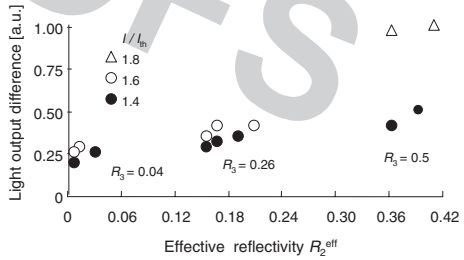

Fig. 9. Light output difference vs. effective reflectivity, R_3 and I/I_{th} as parameters.

L_{ex}, but also on the reflectivity of the LD facet R_1, R_2, and that of the external mirror R_3 and varies with a period of half a wavelength. Light output difference is defined as the difference between the successive light output maximum and the minimum in Fig. 8. Using effective reflectivity $R_2{}^{eff}$, the relationship between the light output difference and $R_2{}^{eff}$, with the drive current I/I_{th} as a parameter is shown in Fig. 9. Light output difference increases as the $R_2{}^{eff}$ increases.

3.2 Wavelength and spectrum characteristics

Wavelength tuning and the spectral behavior due to the strong light feedback is shown in Fig. 10 and Fig. 11, respectively, for the antireflection-coated LD where the drive current (normalized by the threshold current) $I/I_{th} =$

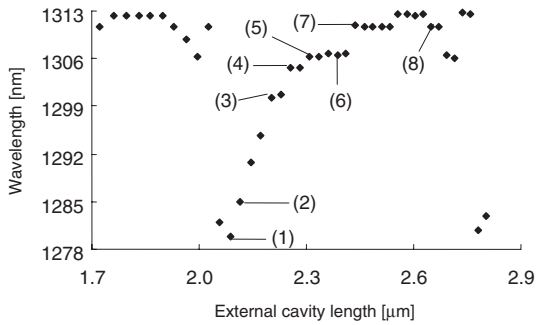

Fig. 10. Dependence of wavelength on external cavity length, where drive current $I/I_{th} = 1.6$, reflectivity $R_1 = 0.32$, $R_2 = 0.01$, and $R_3 = 0.5$.

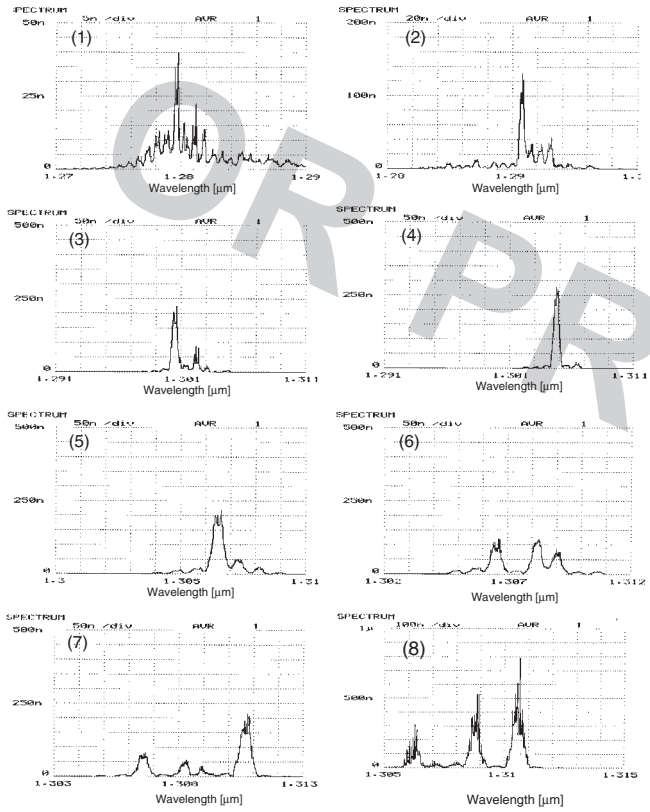

Fig. 11. Spectra at (1), (2), …, and (8) in Fig. 11.

1.8, reflectivity $R_1 = 0.32$, $R_2 = 0.01$, and $R_3 = 0.5$. The wavelength variation exhibits an asymmetric but $\lambda/2$ periodic behavior with the external-cavity length L_{ex}. As the L_{ex} increases the wavelength increases linearly like (1), (2), (3), (4), and (5), then remains like (6), (7), and (8) in every period as shown in Fig. 10.

The spectral structure of the tuned light is shown in Fig. 11 corresponding to the number in Fig. 10. The former (1)–(5) shows that single longitudinal modes are tuned for the feedback light LD, while the latter (6)–(8) shows that multi-modes are tuned for the feedback light LD. Considering these two types of experimental tuning results, we find the spectrum varies from single-mode to multi-mode according to the external cavity length.

The separation between the longitudinal modes by the laser diode's cavity length L is

$$\Delta\lambda = \lambda^2/2n_{eff}L, \tag{3}$$

where n_{eff} is the effective group index of the LD. A calculated mode separation of $\Delta\lambda$ equals 0.76 nm for $\lambda = 1300$ nm, $n_{eff} = 3.7$, and $L = 300\,\mu$m agrees well with the above experimentally obtained result. The span of lasing-mode shifts corresponds to the integral number times $\Delta\lambda$ in Eq. (3).

3.3 *Dependence of wavelength variation on effective reflectivity*

Dependence of wavelength tuning range on the effective reflectivity R_2^{eff}, with I/I_{th} as a parameter is shown in Fig. 12. The wavelength tuning range is defined as the wavelength difference between the successive maximum and the minimum as shown in Fig. 10. Figure 12 shows that the wavelength tuning range increases as the R_2^{eff} increases. The gradient of wavelength (the change of wavelength per external cavity length) also increases as the R_2^{eff} increases, as shown in Fig. 13.

Figure 14 illustrates the typical spectrum structure and a definition of the side-mode suppression ratio ($10\log[a/b]$), spectrum line width (full width half-maximum c) and mode interval (average of d, e, f, and g). The side-mode suppression ratio and mode interval increase as the R_2^{eff} increases, but the spectrum line width decreases as R_2^{eff} increases.

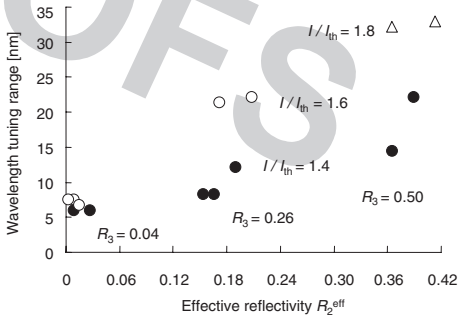

Fig. 12. Dependence of wavelength tuning range on the effective reflectivity R_2^{eff}, with I/I_{th} as a parameter.

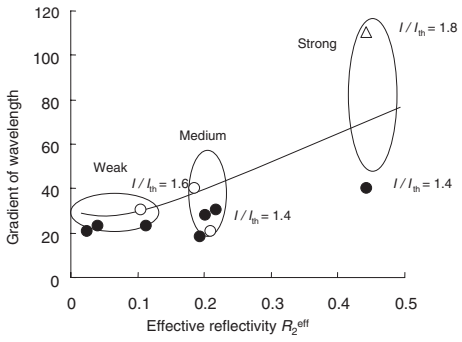

Fig. 13. Relationship between the gradient of wavelength variation and the effective reflectivity R_2^{eff}.

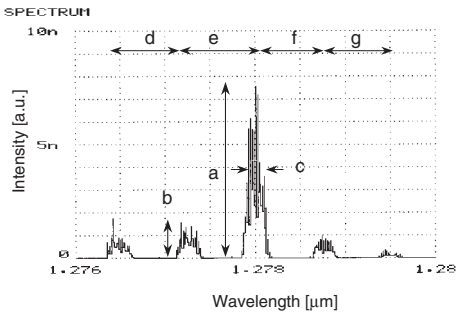

Fig. 14. A definition of side-mode suppression ratio (10 log[a/b]), spectrum line width (full width half-maximum c) and mode interval (average of d, e, f, and g in Fig. 14).

4. Conclusions

A laser diode (LD) attached to a flying slider and a rotating optical disk mirror were used to measure the lasing characteristics for extremely-short-external-cavity LD. Not only the wavelength, but also the spectrum including the side-mode suppression ratio, the spectrum line width and the mode interval could be measured precisely by controlling the slider flying height, with the reflectivities of the LD facets and the external mirror, and the drive current as parameters. As a result, we successfully measured all the parameters related to the light feedback and confirmed a wavelength tuning range as great as 30 nm for a laser diode with an antireflection coating on the facet facing the external mirror. Furthermore, we experimentally analyzed how the parameters of the coupling system affect the extremely-short-external-cavity laser diode's operation. Strongly coupled (low LD facet reflectivity facing an external mirror and high mirror reflectivity) short external cavity length is the key to achieving a wide-range wavelength tuning.

Acknowledgments

The authors would like to thank Mr. Y. Masuda and Mr. S. Ihara of Ritsumeikan University for their help with the experiments. They would also like to acknowledge Mr. H. Nakata of NTT Laboratories for bonding an LD-PD on a slider.

References

1) J. Y. Kim and H. C. Hsieh: J. Lightwave Tech. **10** (1992) 439.
2) P. J. Rodrigo, M. Lim and C. Saloma: Appl. Opt. **40** (2001) 506.
3) J. D. Berger, Y. Zhang, J. D. Grade, H. Lee, S. Hrinya, H. Jerman, A. Fennema, A. Tselikov and D. Anthon: IEEE LEOS Newsletter, Oct. 2001, p. 9.
4) M. C. Larson and J. S. Harris: Appl. Phys. Lett. **68** (1996) 891.
5) F. Sugihwo, M. C. Larson and J. S. Harris: Appl. Phys. Lett. **72** (1998) 10.
6) A. Hsu, J. F. P. Seurin, S. L. Chuang and K. D. Choquette: IEEE J. Quantum Electron. **37** (2001) 1643.
7) Y. Uenishi, M. Tsugai and M. Mehregany: Electr. Lett. **31** (1995) 965.
8) A. Q. Liu, X. Zhang, V. M. Murukeshan, C. Lu and T. H. Cheng: IEEE J. Sel. Top. Quantum Electron. **8** (2002) 73.
9) Y. Sidorin and D. Howe: Appl. Opt. **37** (1998) 3256.
10) P. A. Rupercht and J. R. Brandenberger: Opt. Commun. **93** (1992) 82.
11) Y. Katagiri and H. Ukita: Appl. Opt. **29** (1990) 5074.